Comparative Evaluation of In-Situ Stress Monitoring with Rayleigh Waves

James M. Hughes[1], James Vidler[1], Ching-Tai Ng[2], Aditya Khanna[1], Munawwar Mohabuth[1], L.R. Francis Rose[3], and Andrei Kotousov[1]

[1] School of Mechanical Engineering, The University of Adelaide, SA 5005 Australia

[2] School of Civil, Environmental & Mining Engineering, The University of Adelaide, SA 5005 Australia

[3] Aerospace Division, Defence Science and Technology Group, Fishermen's Bend, VIC 3207, Australia

Abstract: The in-situ monitoring of stresses provides a crucial input for residual life prognosis and is an integral part of structural health monitoring systems. Stress monitoring is generally achieved by utilising the acoustoelastic effect, which relates the speed of elastic waves in a solid, typically longitudinal and shear waves, to the stress state. A major shortcoming of methods based on the acoustoelastic effect is their poor sensitivity. Another shortcoming of acoustoelastic methods is associated with the rapid attenuation of bulk waves in the propagation medium, requiring the use of dense sensor networks. The purpose of this paper is twofold: to demonstrate the application of Rayleigh (guided) waves rather than bulk waves towards stress monitoring based on acoustoelasticity, and to propose a new method for stress monitoring based on the rate of accumulation of the second harmonic of large amplitude Rayleigh waves. An experimental study is conducted using the cross-correlation signal processing technique to increase the accuracy of determining Rayleigh wave speeds when compared with traditional methods. This demonstrates the feasibility of Rayleigh wave based acoustoelastic structural health monitoring systems, which could easily be integrated with existing sensor networks. Second harmonic generation is then investigated to demonstrate the sensitivity of higher-order harmonics to stress induced nonlinearities. The outcomes of this study demonstrate that the sensitivity of the new second harmonic generation method is several orders of magnitude greater than the acoustoelastic method, making the proposed method more suitable for development for online stress monitoring of in-service structures.

Introduction

Online stress monitoring has become an essential component of life prognosis and structural health monitoring (SHM) systems for high-value assets[1]. Stress monitoring can be accomplished by a number of methods which utilise various physical phenomena. One promising technique is based on acoustoelastic phenomena associated with the propagation of guided waves[2]. This technique could be easily integrated with the existing SHM systems, which have been developed recently for detecting and/or sizing of defects in metallic[3,4] and composite structures[5,6]. In general, guided wave-based measurement systems have many practical advantages over existing methods, being light-weight, power efficient, and low cost[7-9].

Guided waves present several novel benefits over conventional bulk-wave inspection techniques[10] and traditional strain gauge methods. Firstly, guided waves are able to propagate longer distances than bulk waves without significant decay[11], which expands the interrogation region and makes inspections more efficient[12-14]. Secondly, guided waves can be judiciously selected to probe for particular types of damage[15]. Guided waves can also be driven in propagation directions that may be inaccessible using conventional ultrasonic evaluation techniques[16]. The two types of guided waves commonly studied are Lamb waves and Rayleigh (surface) waves. The non-dispersive characteristics of Rayleigh waves makes them an attractive candidate for stress measurements relative to Lamb waves as part of an SHM system.

Acoustoelastic effect

The acoustoelastic effect, which describes the dependence of the speed of an elastic wave on the stress state of the medium, received significant attention in the mid 1950's[17,18]. However, the focus has been on the change in bulk wave speeds, rather than guided waves due to difficulties in incorporating the free-surface boundary conditions of such waves into a mathematical model[19]. Dowaikh[20] later expanded the acoustoelastic theory to Rayleigh waves, and derived a relationship describing the change in the velocity of propagating Rayleigh waves with applied stress. Recently, the acoustoelastic theory was extended to Lamb waves in plates[21-23]. However, accurate measurement of the acoustoelastic phenomena of Lamb wave has not been fully achieved experimentally.

The accuracy of stress measurement using the acoustoelastic effect is limited by the resolution of measurement of the elastic wave arrival time[19]. One method of improving the accuracy of stress measurement is to maximise the distance between measurement points. Recent studies on the

acoustoelastic effect have utilised critically refracted longitudinal (LCR) waves to detect stresses in metals and composites at different depths[24,25], with interrogation distances upto 250 mm[24]. This measurement interval is significantly greater than earlier studies, thereby improving the accuracy of stress measurements. Further improvement can be achieved by utilising Rayleigh waves for stress monitoring, which travel at roughly half the speed of longitudinal waves.

Higher order harmonic generation due to material nonlinearity

Another phenomenon which can be used for stress measurement is the dependence of the rate of accumulation of second (and higher-order) harmonics upon the applied stress level[26-28], as indicated schematically in Fig. 1. This is because the generation of higher-order harmonics can be attributed to material nonlinearities including nonlinearities caused by applied, residual, or thermal stresses. This approach has been utilised previously using both guided and bulk waves to detect weak changes in material properties caused by: material degradation[29], fatigue damage in metallic structures[30], plasticity-driven damage in metal plates [12], bonding defects in adhesive joints[31], thermal fatigue in composites[32], damage in concrete structures[33], and radiation damage in reactor pressure vessel steels[34]. Liu[35] applied this approach towards the measurement of surface residual stresses in shot-peened Aluminium specimens, however they could not distinguish the contributions of residual stress and plastic deformation upon the rate of accumulation of the second harmonic. To the best of our knowledge, no attempt has yet been made to show experimentally the effect of applied stresses on the rate of accumulation of the second harmonic.

In general, cumulative generation of higher harmonics requires meeting three internal resonance conditions: (i) matching of the phase velocity; (ii) matching of the group velocity; and (iii) nonzero power flux from the fundamental amplitude to the higher-order harmonics[36]. Satisfying these conditions can only occur at certain values of frequency-thickness for Lamb waves[37]; however, they are automatically satisfied for Rayleigh waves because of their non-dispersive nature. This makes them an attractive candidate for conducting stress measurements. Moreover, the weak nonlinearity effect of metallic waveguides results in small amplitudes of higher-order harmonics that is often difficult to detect. Rayleigh waves maximise the observability of nonlinear effects, as their high-power density near the surface of the waveguide results in significantly stronger nonlinear effects than that observed for bulk waves[38]. Finally, complications with dispersion and the multi-modal nature of Lamb waves can cause errant results[12], which are avoided with Rayleigh waves due to their nondispersive characteristics. Detection of the Rayleigh wave is usually achieved using a non-

contact method, as coupling conditions directly influence the consistency and repeatability of second harmonic generation (SHG) experiments[26]. Hence, the scanning laser vibrometer utilised in the present work is a suitable tool for stress measurement using the second harmonic generation method.

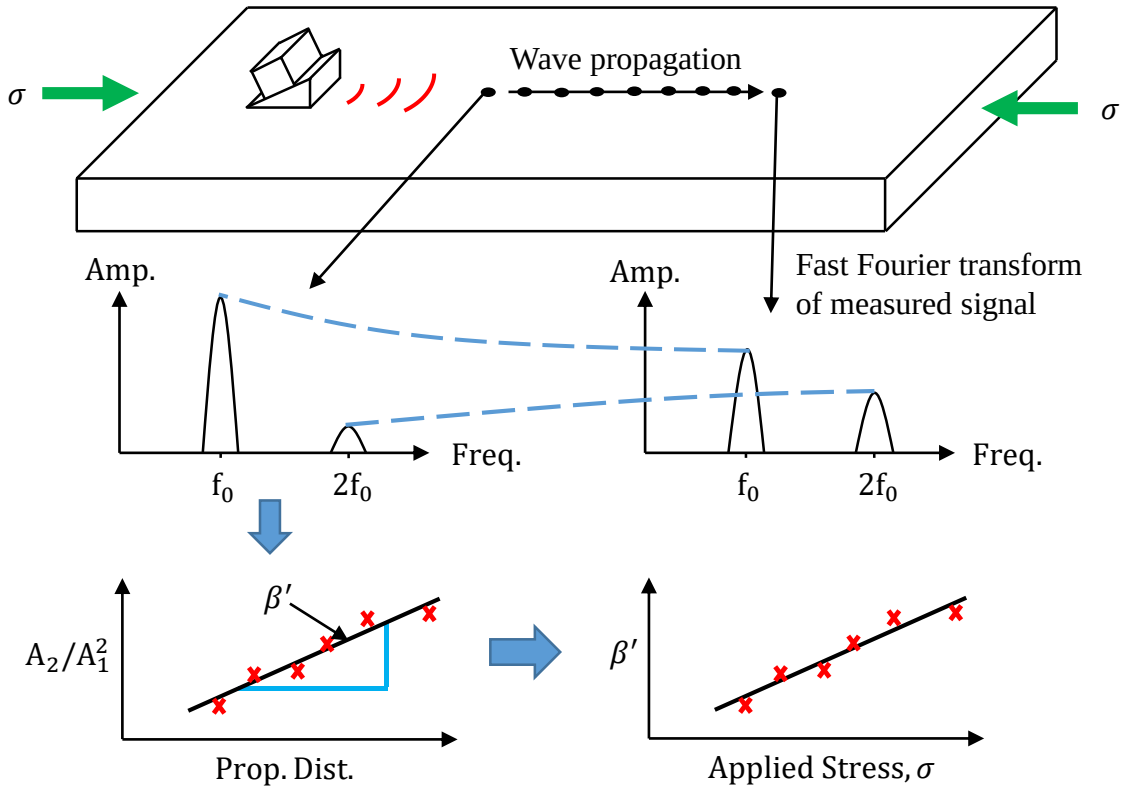

Fig. 1. Schematic showing the relative growth of the second harmonic relative to the fundamental with propagation distance.

The current study provides a comparative evaluation the acoustoelastic effect and SHG for estimating applied stresses with nonlinear Rayleigh waves. The study first focuses on the acoustoelastic effect. A systemic and robust measurement approach is proposed to improve the accuracy and reliability in determining the wave speed by using cross-correlation of Rayleigh wave signals, which can ultimately be used to measure applied stresses. Second harmonic generation is then investigated to determine its suitability as an alternative stress monitoring method. The performance of both techniques in assessing the change of the applied stress is investigated. The findings of this study provide fundamental insights into the suitability and accuracy of using nonlinear Rayleigh wave techniques in stress monitoring.

The structure of the paper is as follows. The theoretical background for the acoustoelastic effect and SHG is presented in the following section. The experimental methodology is then discussed, which covers the generation, measurement, and signal processing associated with Rayleigh waves and the two measurement techniques. Experimental results are presented for both stress measurement methods (acoustoelasticity and SHG), and the methods are critically compared to evaluate their effectiveness. Suggestions for future research are then explored and the key findings are presented.

Theoretical Background

Acoustoelastic theory

As mentioned in the previous section, the relationship between bulk wave velocities and applied stress was first presented by Hughes and Kelly[17]. In the notations of Rose[39], the effect of an applied uniaxial stress on longitudinal and shear wave velocities can be expressed as:

$$\rho_0 V_{113}^2 = \lambda + 2\mu + \frac{\sigma}{3\kappa_0}\left[2l - \frac{2\lambda}{\mu}(\lambda + 2\mu + m)\right], \tag{1}$$

$$\rho_0 V_{132}^2 = \mu + \frac{\sigma}{3\kappa_0}\left[m - \frac{\lambda + \mu}{2\mu}n - 2\lambda\right], \tag{2}$$

$$\rho_0 V_{133}^2 = \mu + \frac{\sigma}{3\kappa_0}\left[m - \frac{\lambda}{4\mu}n + \lambda + 2\mu\right], \tag{3}$$

where V_{113}, V_{132}, and V_{133} are the longitudinal wave speed propagating perpendicular to the applied stress, the shear wave speed polarised perpendicularly and travelling perpendicular to the applied stress, and the shear wave speed polarised parallel and travelling perpendicular to the applied stress respectively, ρ_0 is the density in the stress-free state, λ and μ are the Lame constants, κ_0 is the stress-free bulk modulus, σ is the value of the applied stress, and $l, m,$ and n are the Murnaghan (third order) elastic constants[10]. Equations (1), (2), and (3) can be inverted to evaluate the elastic constants from wave velocity measurements and applied stresses.

In the case of Rayleigh waves, the change of the wave velocity can be found from a characteristic equation presented by Dowaikh[20], which can be written as:

$$\alpha_{22}(\alpha_{11}-\rho_0c^2)[\gamma_2(\gamma_1-\rho_0c^2)-(\gamma_2-\tau_2)^2] = [\alpha_{12}^2+\alpha_{22}(\rho_0c^2-\alpha_{11})][\alpha_{22}\gamma_2(\alpha_{11}-\rho_0c^2)(\gamma_1-\rho_0c^2)]^{\frac{1}{2}}, \quad (4)$$

where $\alpha_{11}=\mathcal{JA}_{01111}$, $\alpha_{22}=\mathcal{JA}_{02222}$, $\alpha_{12}=\mathcal{JA}_{01122}$, $\gamma_1=\mathcal{JA}_{01212}$, $\gamma_2=\mathcal{JA}_{02121}$, τ_2 is the stress in the x_2 direction, c is the wave speed, and ρ_0 is the stress-free density. A full description of the instantaneous elasticity tensor components $\mathcal{JA}_{0ijkl}$ can be found in Dowaikh[20]. The solution to this equation provides an approximately linear relationship between Rayleigh wave speed and the applied stress for stresses below the yield, as shown in Fig. 2. Experimental wave speed data can therefore be correlated to the stress applied to the wave guide using a linear trend line, and in this manner stress measurement can be achieved.

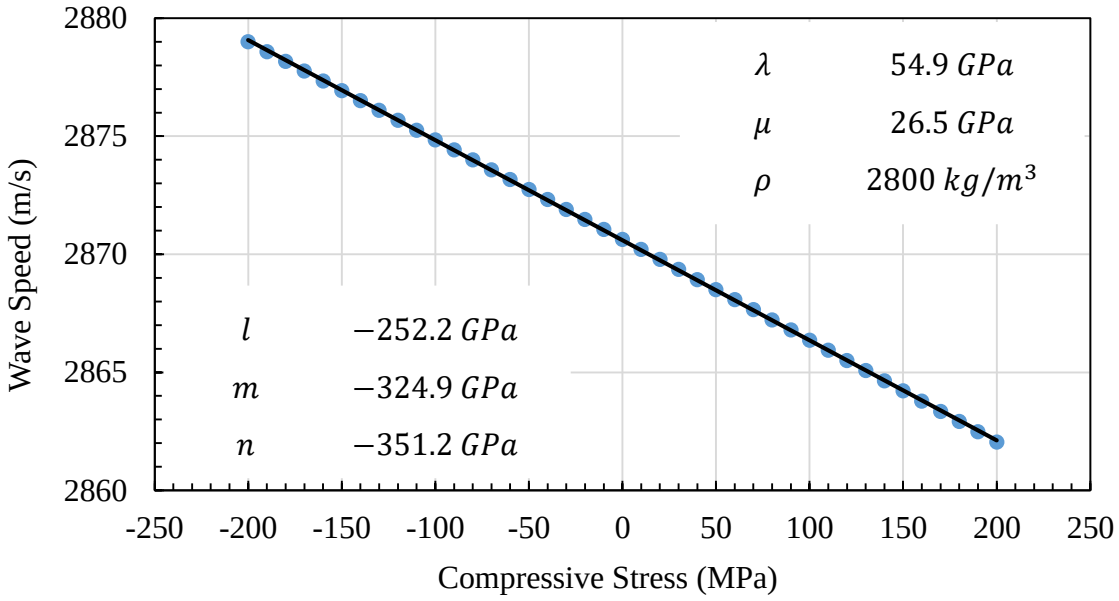

Fig. 2. Solution to Eq. (4) between ± 200 MPa for Aluminium 7075-T651, using material constants presented by Muir[40].

Second-harmonic generation theory

The growth in amplitude of the second harmonic for nondispersive waves can be derived for one-dimensional wave propagation governed by the equation[22]:

$$\rho\frac{\partial u^2}{\partial t^2}=\frac{\partial \sigma}{\partial x}, \quad (5)$$

where ρ is the density of the material through which the wave propagates, u is the particle displacement, and σ is the normal stress. Assuming weak quadratic nonlinearity, the nonlinear form of Hooke's law can be written:

$$\sigma = E\varepsilon + E\beta\varepsilon^2 \,, \tag{6}$$

where E is the modulus of elasticity, $\varepsilon = \partial u/\partial x$ is the strain, and β is a measure of the quadratic nonlinearity of the material, called the nonlinearity parameter. Combining Eqs. (5) and (6) leads to:

$$\rho \frac{\partial u_x^2}{\partial t^2} = E \frac{\partial^2 u}{\partial x^2} + 2E\beta \frac{\partial^2 u}{\partial x^2} \,, \tag{7}$$

A perturbation solution of the second order can be derived for Eq. (7) and takes the form[22]:

$$u = A_1 \, cos(kx - \omega t) - A_2 sin2(kx - \omega t), \tag{8}$$

where A_1 is the amplitude of the fundamental frequency and A_2 is the amplitude of the second harmonic generated due to material nonlinearity. The perturbation analysis then leads to the following relation[41]:

$$A_2 = \frac{\beta}{8} A_1^2 \kappa^2 x \,, \tag{9}$$

where $\kappa = \omega/c$ is the wavenumber and x is the propagation distance. Equation (9) shows a dependence between the nonlinearity parameter (β) and the normalised second harmonic (A_2/A_1^2), which also extends to Rayleigh waves[26].

The particle displacement normal to the surface for the fundamental and second harmonic components of a Rayleigh wave is presented in Thiele[42], as follows:

$$u_z(\omega_0) = iA_1 \frac{b_1}{\kappa_R} \left(e^{b_1 z} - \frac{2\kappa_R^2}{\kappa_R^2 + b_2^2} e^{b_2 z} \right) exp[i\kappa_R (x - c_R t)] \,, \tag{10}$$

$$u_z(2\omega_0) \approx iA_2 \frac{b_1}{\kappa_R} \left(e^{2b_1 z} - \frac{2\kappa_R^2}{\kappa_R^2 + b_2^2} e^{2b_2 z} \right) exp[i2\kappa_R (x - c_R t)] \,, \tag{11}$$

where $b_1^2 = \kappa_R^2 - \kappa_L^2$ and $b_2^2 = \kappa_R^2 - \kappa_T^2$. Here, κ_R, κ_L, and κ_T represent the wavenumbers of the Rayleigh wave, longitudinal wave, and shear wave in the material. Hermann4[3] presented the nonlinearity parameter of a propagating Rayleigh wave in terms of the fundamental and second harmonic components at the surface (where $z = 0$):

$$\beta = \frac{u_z(2\omega_0)}{u_z^2(\omega_0)x}\frac{i8b_1}{\kappa_L^2\kappa_R}\left(1 - \frac{2\kappa_R^2}{\kappa_R^2 + b_2^2}\right), \tag{12}$$

In practice, it is more common to measure the relative nonlinearity parameter (RNLP), β' which is proportional to the nonlinearity parameter[10,27,28,35]:

$$\beta' = \frac{A_2}{A_1^2 x}, \tag{13}$$

Hence, β' can be determined by measuring the fundamental and second harmonic amplitudes at a number of distances along the direction of Rayleigh wave propagation and determining the gradient of the line of best fit, as indicated schematically in Fig. 1. As it is known that the rate of accumulation of the second harmonic is dependent on the nonlinearity of the waveguide[26], it is possible to correlate the nonlinearity parameter to the stress applied to the waveguide by measuring β' at various stress levels and comparing this to existing theoretical and experimental data. The aim of this paper is therefore to (i) investigate the feasibility of stress measurement using the acoustoelastic effect and SHG, and (ii) to compare the effectiveness of these methods.

Experiment

Generation of Rayleigh waves

A Rayleigh wave is typically generated by using a wedge to refract a longitudinal wave generated by an ultrasonic transducer into a Rayleigh wave in the specimen[44]. The angle of the wedge must be calculated using Snell's law (Eq. 14) to ensure that most of the energy is concentrated into the Rayleigh wave.

$$\theta_w = \sin^{-1}\left(\frac{c_{L,w}}{c_R}\right), \tag{14}$$

where θ_w is the wedge angle, $c_{L,w}$ is the longitudinal wave velocity in the wedge material, and c_R is the Rayleigh wave velocity in the specimen.

It is important to minimise the generation of shear waves in the specimen, as the shear and Rayleigh wave speeds are usually similar and can interfere with TOF and SHG measurements. Many past experiments have utilised the wedge excitation method to generate Rayleigh waves in metallic specimens[10,27,35,42,45]. This work uses a high density polyethylene wedge of angle $\theta_w = 52°$ to generate Rayleigh waves in an aluminium specimen, as shown in Fig. 3. The wedge, transducer, and specimen are acoustically coupled using ISO68 oil and a firm clamping pressure at both the wedge-specimen and transducer-wedge interfaces. The wedge is not removed between tests to mimimise the measurement error[26].

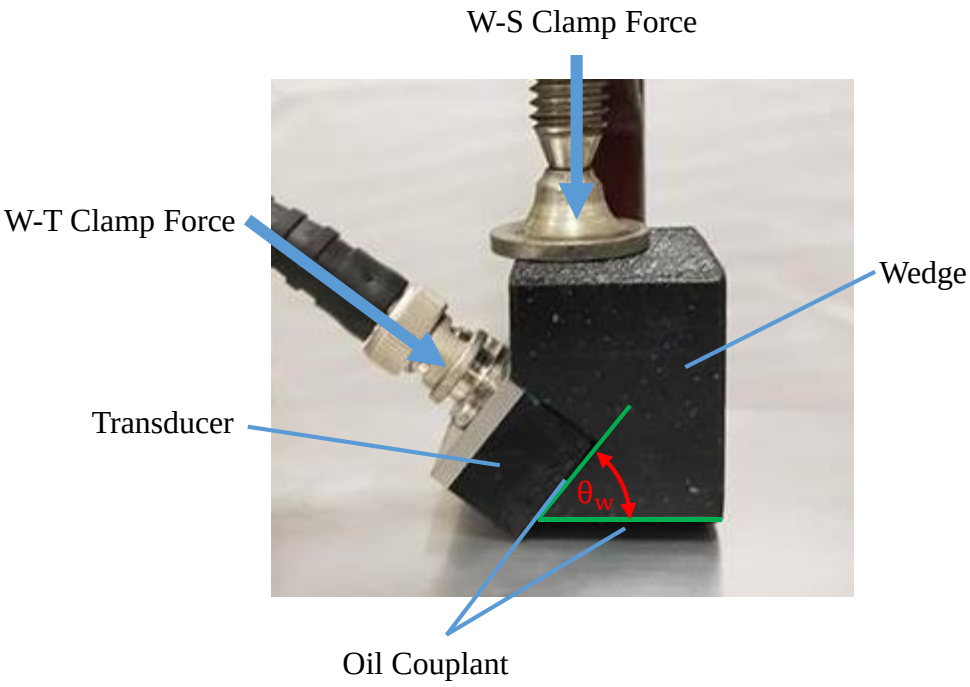

Fig. 3. Wedge-transducer-specimen assembly.

Specimen preparation and measurement methodology

A schematic of the experimental setup is shown in Fig. 4. A Tektronix AFG 3021B arbitrary function generator is used to generate a 1 MHz, 12-cycle sine-windowed sinusoidal tone burst. The number of cycles in the tone burst is selected to provide a good compromise between frequency and time resolution. The tone burst is amplified to approximately 700 V peak-to-peak by a RITEC GA-2500A gated amplifier – as used by Thiele[42] to reduce nonlinear amplification effects on measurements – and is sent to a 1 MHz Olympus longitudinal transducer coupled to the wedge. The wavelength of the Rayleigh wave is $\lambda_R = 2.9$ mm, which is significantly smaller than the thickness

of the aluminium specimen (dimensions $l = 416.5$ mm, $w = 183.5$ mm, $t = 47.5$ mm) and ensures that the Rayleigh wave generation conditions are satisfied. The Rayleigh wave amplitude is measured at multiple positions on the Aluminium specimen using a Polytec PSV-400-M2-20 scanning laser vibrometer, which uses a band pass filter between 200 kHz and 10 MHz to reject low- and high-frequency noise. The laser vibrometer detection is advantageous for a number of reasons: (i) it provides non-contact detection; (ii) it has a flat frequency response; and (iii) it has a high sampling frequency of 102.4 MHz. The compressive force (F_c) is provided by an Avery Universal Testing Machine, and is far lower than the theoretical buckling load for the specimen. The specimen is prepared by polishing the surface with 1200-grit sandpaper to achieve a consistent, reflective finish, which has been shown to increase the accuracy of laser vibrometer measurements[46]. The experimental setup is shown in Fig. 5.

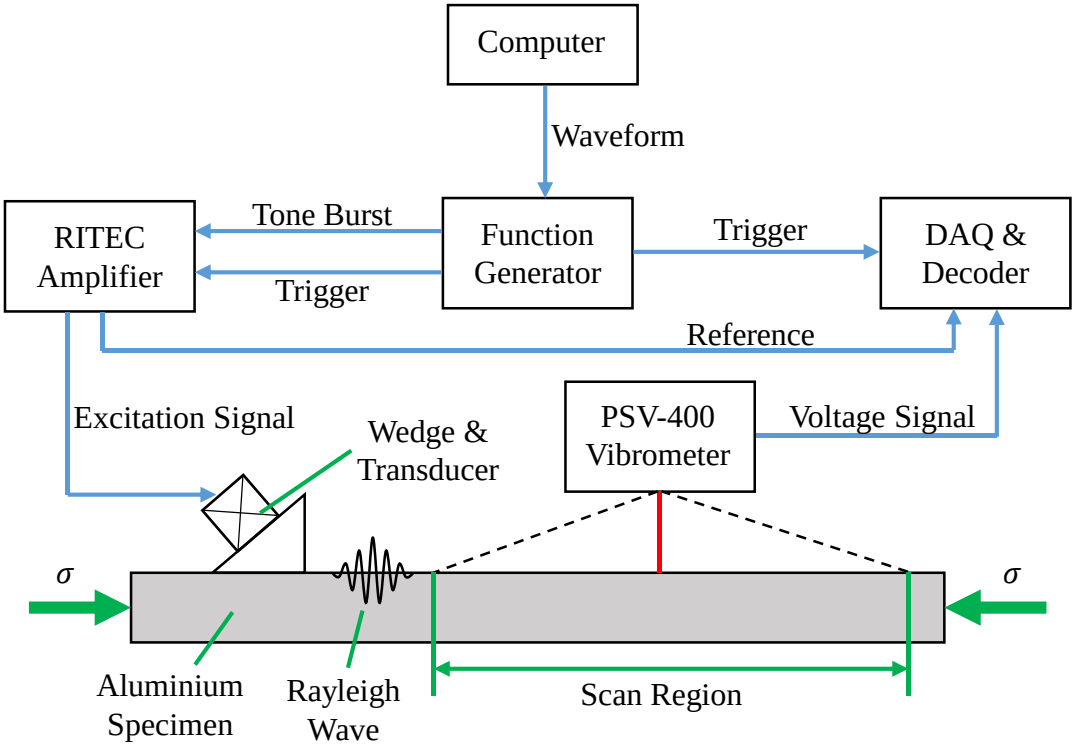

Fig. 4. Schematic of the experimental setup, indicating the wave generation, applied stress and other instrumentation.

Fig. 5. Experimental setup showing the specimen and loading frame as well as the head of the scanning laser vibrometer.

Measurement of the change in wave speed

The out-of-plane Rayleigh wave amplitude is measured at nine locations along the surface of the Aluminium specimen, which are arranged in three groups of three, as shown in Fig. 6. The received signal is averaged 4000 times to improve the signal-to-noise ratio, as past experiments suggest increasing the number of averages will result in more reliable measurements[46]. Cross-correlation is used to determine the time lag between point one and the other eight points, which gives the time of arrival of the Rayleigh wave along the specimen. Given the known distances between the points, a regression line can be fitted between the time lag vector and the distances vector, the slope of which is the Rayleigh wave speed.

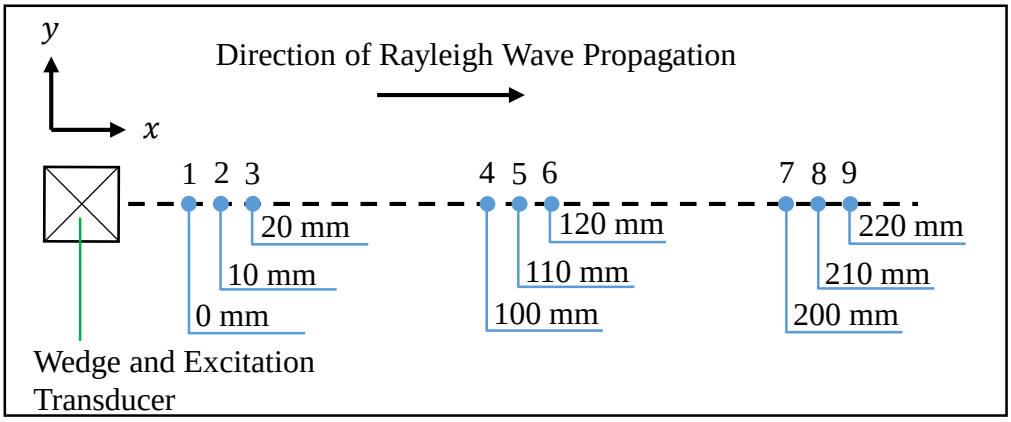

Fig. 6. Rayleigh wave measurement locations

A brief overview of cross-correlation is now presented as described by Allen and Mills[47]. Cross-correlation is a technique that can be used to accurately determine the time lag between two separate signals with common features. Consider two discrete time domain signals of length n which take the form $X = (x_1, x_2, \dots, x_n)$ and $Y = (y_1, y_2, \dots, y_n)$ where the common time vector is $T = (t_1, t_2, \dots, t_n)$. It is assumed that both X and Y contain the same finite duration waveform $W = (W_1, W_2, \dots, W_i)$ for $i < n$ separated by some time lag, k. It is then possible to write:

$$W_1 = x_j = y_{j+k}\,, \tag{15a}$$

$$W_2 = x_{j+1} = y_{j+k+1}\,, \tag{15b}$$

and so on. The cross-correlation function determines the time lag k between the two time domain signals by comparing all possible time lags and minimising the error. This is achieved by first defining the l^2 norm function as $d(X,Y) = \|X - Y\|_2$. The time lag k is then minimised when $d(X,Y)$ is minimised, which leads to:

$$\|X - Y\|_2^2 = \|X\|^2 + \|Y\|^2 - 2\langle X, Y\rangle\,, \tag{16}$$

where $\langle X, Y\rangle$ is the inner product. It is clear that for finite signals X and Y, this minimisation occurs when the inner product is maximised. The inner product can be written as:

$$y(k) = \langle X, Y\rangle = \sum_{p=k}^{n} X(p-k)Y(p)\,, \tag{17}$$

Hence, the maximum correlation between the two signals can be found when $y(k)$ is maximised.

In this study, two methods for TOF determination are used: the cross-correlation method and a simpler method in which the average arrival time of the signal maxima and minima are used to determine the TOF. Eleven values of compressive force are applied to the Aluminium specimen between 200 kN and 300 kN in 10 kN increments, giving a compressive stress range between 22.9 MPa and 34.4 MPa.

Measurement of the growth of the second harmonic

The use of a wedge to generate Rayleigh waves greatly reduces the component of bulk waves present in the specimen, and the Rayleigh wave can therefore be identified as the largest amplitude wave-packet. Confirmation of Rayleigh wave generation is also achieved by ensuring that the measured wave speed is similar to the theoretical wave speed. The frequency components of the signal at each of the measurement points are extracted by performing a fast Fourier transform (FFT) on the Rayleigh wave component of the measured signal. The latter is extracted by applying a rectangular window of width 12μs centered at the Rayleigh wave arrival time to the measured signal. The amplitude of the FFT is determined using a root-mean-square (RMS) method between $\pm$0.1 MHz for the fundamental frequency and $\pm$0.15 MHz for the second harmonic. Figure 7 shows a typical time-domain signal for measurement location 4, and Fig. 8 shows the resulting FFT.

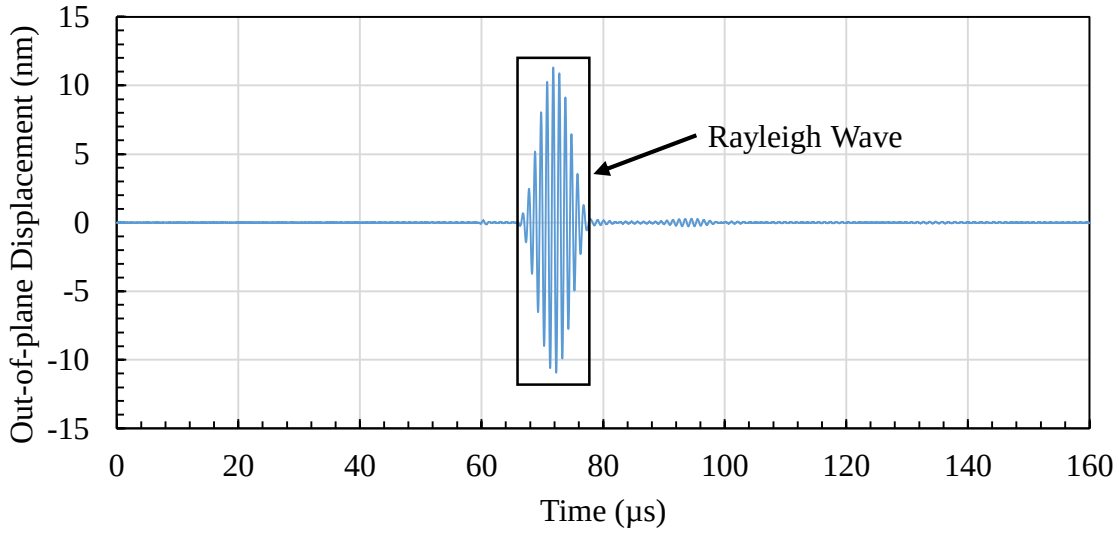

Fig. 7. Received time domain signal at point 4 in Fig. 5, under 250 kN compressive load.

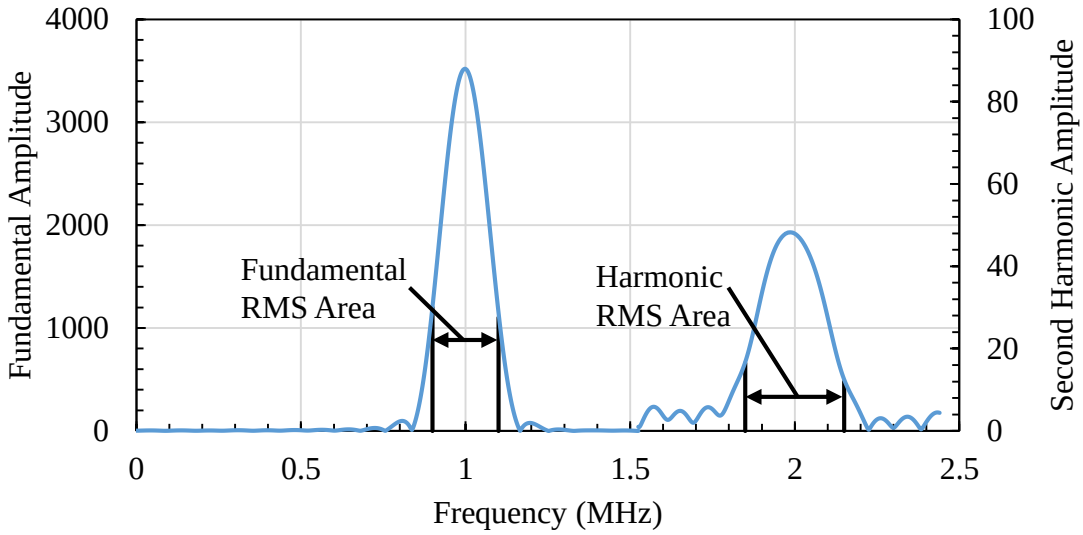

Fig. 8. Fast Fourier transform of received signal, showing the fundamental and second harmonic components of the nonlinear Rayleigh wave.

Test Results and Discussion

Change of velocity

Figure 9 shows the arrival time at the nine measurement locations using cross-correlation at a compressive stress of 28.7 MPa. This measurement is normalised to the first data point, and a least squares regression line is fitted to determine the speed of the Rayleigh wave. Figures 10 and 11 demonstrate the drastic influence signal processing methods have on the results. It should be noted that the 24.1 MPa measurement has been omitted due to an obvious error that may be attributed to a small misalignment of the specimen, and the 22.9 MPa measurement was used to accurately determine the distances between measurement locations. The conventional approach to TOF data processing, as previously described, shows very poor correlation between the Rayleigh wave speed and the applied stress ($R^2 = 0.35$). However, the trend between wave speed and applied stress is very evident when a cross-correlation approach is used. The R^2 value of 0.91 suggests that there is a strong correlation between the applied stress and the speed of the Rayleigh wave. The cross-correlation method also produced a smaller average standard error ($0.19\ m/s$) than the traditional method ($0.31\ m/s$), indicating a significant improvement. Therefore, it is possible to use Rayleigh waves for practical in-situ stress monitoring with the acoustoelastic effect.

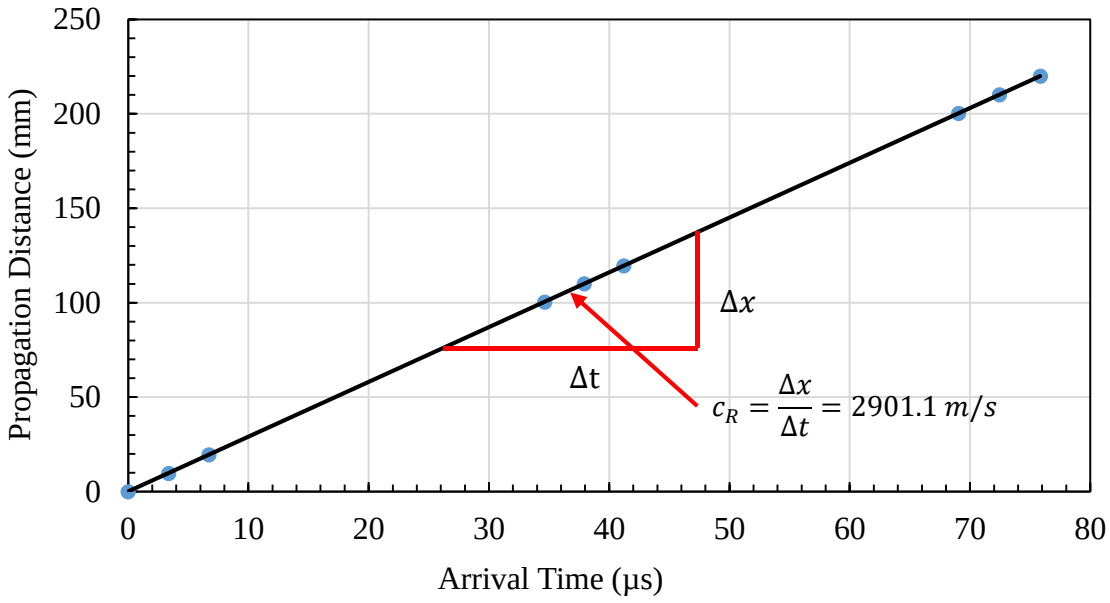

Fig. 9. Rayleigh wave speed against applied compressive stress using traditional signal processing methods.

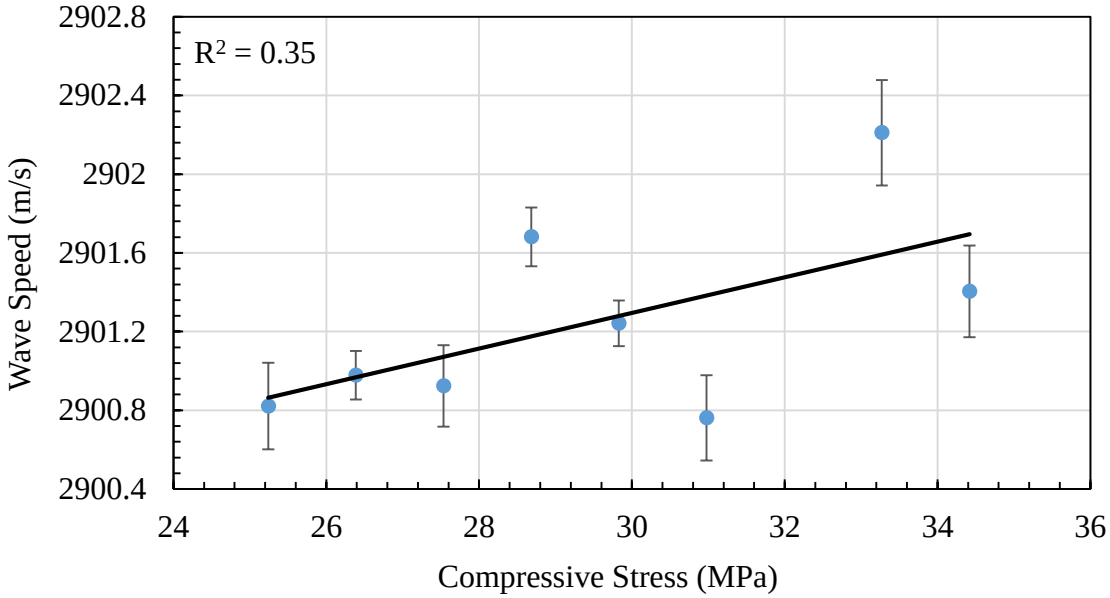

Fig. 10. Rayleigh wave speed against applied compressive stress using traditional signal processing methods.

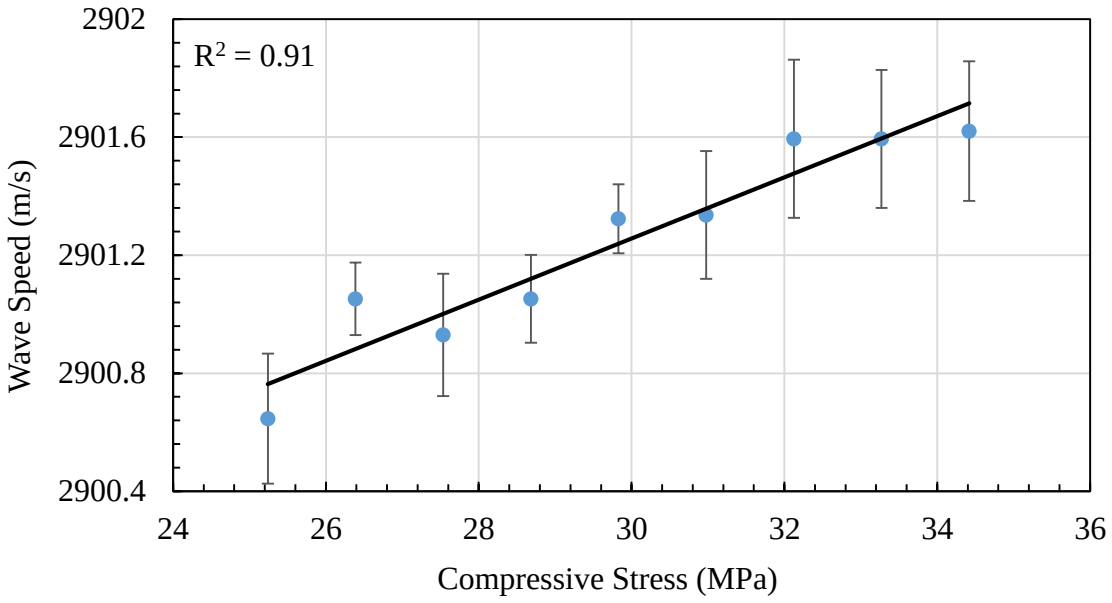

Fig. 11. Rayleigh wave speed against applied compressive stress using cross-correlation to determine the time-of-flight.

Growth of the second harmonic

Figure 12 displays the relationship between the normalised second harmonic and propagation distance for an applied stress of 26.4 MPa. It should be noted that no diffraction or attenuation corrections were performed on the signal as these can be considered negligible for small propagation distances[14]. It is known from Eq. 12 that the relationship between the normalised second harmonic (A_2/A_1^2) and propagation distance is linear, which is supported by the data gathered during this research and many other studies[24,27,42,45], which have investigated the unstressed nonlinearity of aluminium specimens. Least squares regression lines for order one and two polynomials are fitted to the data to determine the relationship between the applied stress and β', which is shown for different applied stress levels in Fig. 13. It is clear that there is an increasing trend in material nonlinearity with applied compressive stress.

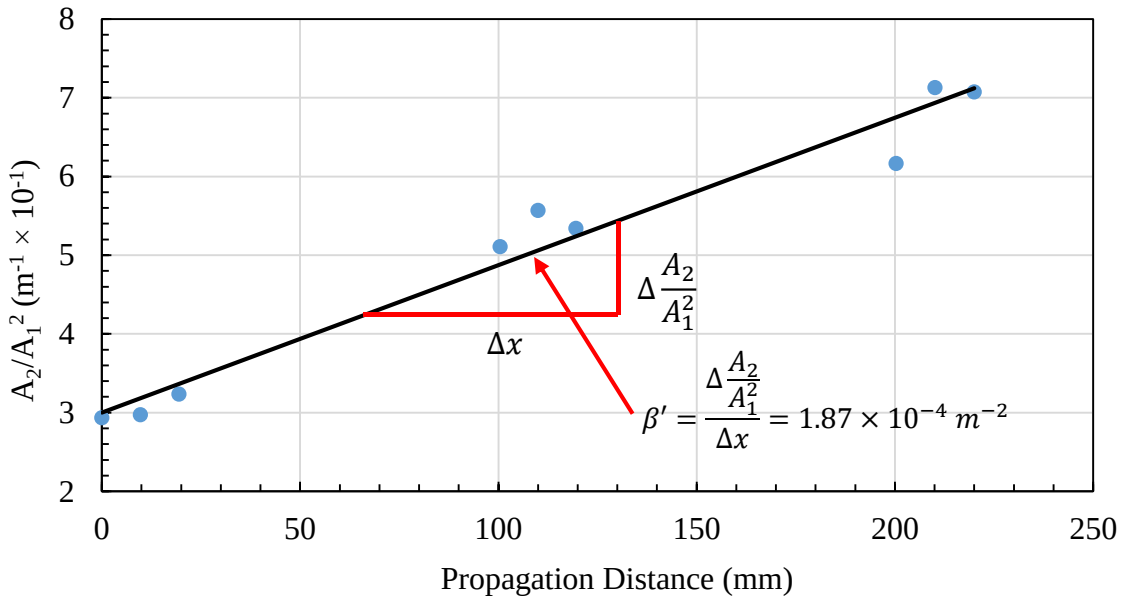

Fig. 12. Normalised second harmonic against propagation distance at a compressive stress of 26.4 MPa.

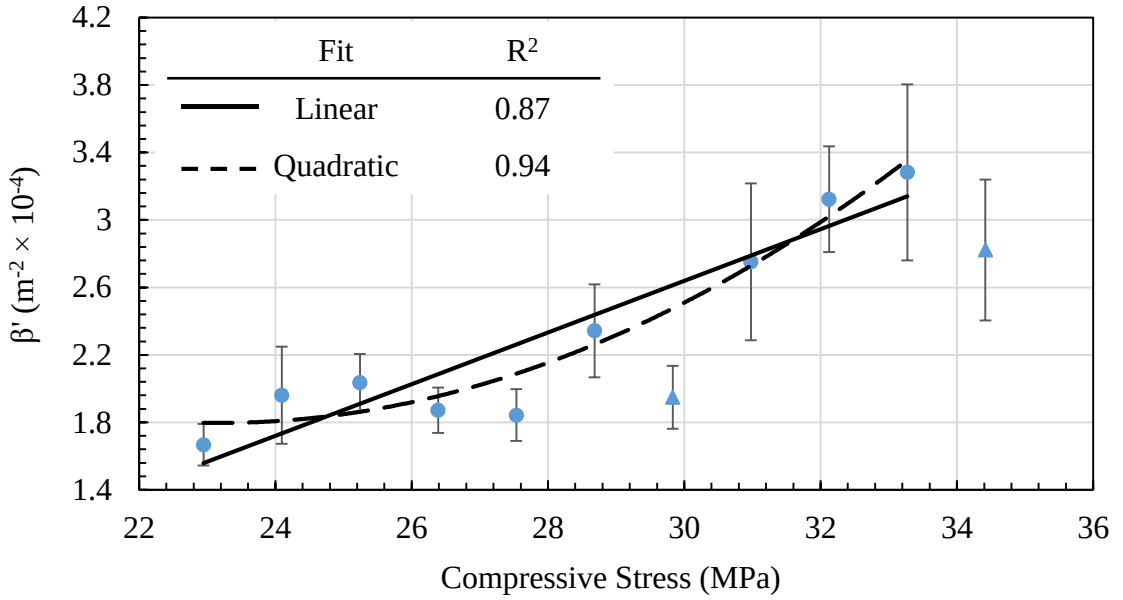

Fig. 13. Change in the β′ against applied compressive stress.

It can be seen that the SHG method experiences a larger scatter of the data than the acoustoelastic method. Two outliers in the data have also been identified, and can be distinguished in Fig. 10 as triangular points. The data gathered suggests that the sensitivity of the SHG method is far higher

than the acoustoelastic method. Using the linear fitted curves between 22 MPa and 32 MPa, the SHG method experiences a 116% increase, while the change in wave speed is only 0.036%, indicating the future potential of such a method for accurate stress monitoring. However, it is evident from this study that although the SHG method is vastly more sensitive than acoustoelastic methods, current measurement techniques are unable to measure the growth of the second harmonic accurately and consistently enough to use this method to determine applied stresses. Future experiments are required to further investigate more fully the relationship between applied stresses and the growth of higher-order harmonics in metallic specimens.

Comparison with Recent Developments

There have been significant advancements to stress evaluation techniques in recent years, many of which are focused on providing non-destructive, in-situ stress monitoring of structures. Notably, stress monitoring using critically refracted longitudinal (Lcr) waves and ultrasonic shear wave spectral analysis (SWSA) have received recent attention. One advantage of Lcr waves over Rayleigh waves (as used in this study) is their greater sensitivity to stress[24,48,50]. However, the higher speed of longitudinal waves makes TOF measurements difficult, whereas slower Rayleigh waves can be measured with greater relative accuracy. Some studies have found that this limits the usefulness of Lcr based methods to changes in stress of over 100 MPa[49]. Further investigation is required in regards to the accuracy of Rayleigh wave based acoustoelastic stress monitoring methods. An advantage of Rayleigh waves over Lcr waves is the theoretically higher interrogation range. This occurs as the energy of a Rayleigh wave is concentrated at the surface, as well as the increased scattering of bulk waves[48]. Studies have found the stability and repeatability of Lcr wave measurements allows accurate determination of uniaxial stresses over lengths as small as 5mm[24]. Similar to Rayleigh waves, the frequency-depth dependence of Lcr waves allows stress interrogation at different depths below the surface of the structure[24].

Shear wave spectral analysis has recently been proposed as a method for stress evaluation of in-situ structures. Similar to the methods proposed in this study, SWSA allows for single sided interrogation, which is advantageous for real world applications. This technique does not require accurate TOF information to determine stresses – which is a major downfall of acoustoelastic based methods – rather it uses the birefringence of shear waves to determine stress[51], which may provide more reliable stress information. Similar to acoustoelastic based methods, SWSA relies on extensive

calibration before implementation, which is often difficult to achieve for in-situ structures[51]. Additionally, the SWSA method is affected by material fatigue, corrosion, and damage, which may limit its longevity for real world applications.

Second harmonic generation presents an interesting opportunity for in-situ stress monitoring. Its major advantage over current methods is the higher sensitivity of SHG to applied stresses, as shown in this study. However, the large scatter associated with the results gained implies that although this method has the potential for use in stress monitoring, further work is required to increase the measurement accuracy. Additionally, the current work utilised a laser vibrometer measurement system, which is not practical for in-situ applications; further research is required to develop a reliable measurement system for in-situ applications. The benefits of SHG over the Lcr and SWSA methods invites further investigation into the possibility of using such a method for future stress monitoring applications.

Conclusion

The use of Rayleigh waves for stress monitoring applications is highly desirable due to their long propagation distance, sensitivity to stresses, and nondispersive nature. The current work has shown that the acoustoelastic effect may be utilised for measurement of stresses applied to an Aluminium specimen with Rayleigh waves. The experimental data shows high correlation between the speed of a Rayleigh wave and the applied stress, indicating that acoustoelasticity with Rayleigh waves may be used for online monitoring of stresses. The use of cross-correlation as a means of determining the time-of-flight of a Rayleigh wave was also shown to improve the accuracy of acoustoelastic techniques. The effect of stresses on second harmonic generation was also investigated, and a clear increasing trend between applied compressive stress and the β' was shown. The results indicate that the sensitivity of the second harmonic generation method is far larger than the acoustoelastic effect, however, difficulties with measurement scatter must be improved before this method becomes viable for monitoring for stresses. Overall, the results obtained in this research demonstrate the feasibility of using Rayleigh waves and various phenomena for stress monitoring, which could be integrated with existing SHM systems.

Acknowledgements

This work was supported by the Australian Research Council through Discovery Project DP160102233 and the Australian Government Research Training Program Scholarship. Their support is greatly appreciated. The authors would also like to thank Johanna Chambrey, Melanie Leroyer-Fortin, and Martin Bertin for their extensive support with laboratory work.

References

1. Croxford AJ, Wilcox PD, Drinkwater BW, et al. Strategies for guided-wave structural health monitoring. *Proc R Soc Lond* 2007; 463: 2961-2981.
2. Pau A and di Scalea FL. Nonlinear guided waves in prestressed plates. *J Acoust Soc Am* 2015; 137: 1529-1540.
3. He S and Ng CT. Guided wave-based identification of multiple cracks in beams using a Bayesian approach. *Mech Syst Sig Process* 2017; 84: 324-345.
4. Mariani S, Nguyen T, Phillips RR, et al. Noncontact ultrasonic guided wave inspection of rails. *Struct Health Monitor* 2013; 12: 539-548.
5. Haynes C, Todd M, Nadabe T et al. Monitoring of bearing failure in composite bolted connections using ultrasonic guided waves: A parametric study *Struct Health Monitor* 2013; 13: 94-105.
6. Soleimanpour R and Ng CT. Locating delaminations in laminated composite beams using nonlinear guided wave. *Eng Struct* 2017; 131: 207-219.
7. Duquennoy M, Ouaftouh M, Ourak M, et al.Theoretical determination of Rayleigh wave acoustoelastic coefficients: comparison with experimental values. *Ultrasonics* 2002; 39: 575-583.
8. Liu P, Lim HJ, Yang S, et al. Development of a “stick-and-detect” wireless sensor node for fatigue crack detection. *Struct Health Monitor* 2016; 16: 153-163.
9. Soleimanpour R, Ng CT and Wang CH. Higher harmonic generation of guided waves at delaminations in laminated composite beams. *Struct Health Monitor* 2017; 16:400-417.
10. Thiele S. Air-Coupled Detection of Rayleigh Surface Waves to Assess Material Nonlinearity due to Precipitation in Alloy Steel. Master’s Thesis, Georgia Institute of Technology, USA, 2013.
11. Achenbach JD. *Wave Propagation in Elastic Solids*. Amsterdam: North-Holland Publishing Company, 1973, pp.187-193.
12. Pruell C, Kim J-Y, Qu J, et al. Evaluation of fatigue damage using nonlinear guided waves. *Smart Mater Struct* 2009; 18: 1-7.
13. Rose JL. *Ultrasonic Guided Waves in Solid Media*. New York: Cambridge University Press,2014, p.3.

14. Ng CT. On accuracy of analytical modeling of Lamb wave scattering at delaminations in multilayered isotropic plate. *Int J Struct Stab Dyn* 2015; 15: 1540010.
15. Wilcox PD, Lowe MJS and Cawley P. Mode and transducer selection for long range Lamb wave inspection. *J Intell Mater Syst Struct* 2001; 12: 553-565.
16. Doherty C and Chui WK. Scattering of untrasonic-guided waves for health monitoring of fuel weep holes. *Int J SHM* 2012; 11: 27-42.
17. Hughes DS and Kelly JL. Second-Order Elastic Deformation of Solids. *Phys Rev* 1953; 92: 1145-1149.
18. Murnaghan FD. Finite Deformations of an Elastic Solid. *Am J Math* 1937; 52: 235-260.
19. Jassaby K and Kishoni D. Experimental Technique for Measurement of Stress-acoustic Coefficients of Rayleigh Waves. *Exp Mech* 1983; 23: 74-80.
20. Doawikh MA. Surface and Interfacial Waves and Deformations in Pre-Stressed Elastic Materials. PhD Thesis, University of Glasgow, UK, 1990.
21. Gandhi N, Michaels JE and Lee SJ. Acoustoelastic Lamb wave propagation in biaxially stressed plates. *J Acoust Soc Am* 2012; 132: 1284-1293.
22. Mohabuth M, Kotousov A and Ng CT. Effect of uniaxial stress on the propagation of higher-order Lamb wave modes. *Int J Nonlinear Mech* 2016; 86: 104-111.
23. Mohabuth M, Kotousov A, Ng CT and Rose LRF. Implication of changing loading conditions on structural health monitoring utilizing guided waves. *Smart Mater Struct* 2018; 27: 025003.
24. He J, Li A, Teng J, et al. Absolute stress field measurement in structural steel members using the Lcr wave method. *Meas* 2018; 122: 679-987.
25. Wang W, Zhang Y, Zhou Y, et al. Plane stress measurement of orthotropic materials using critically refracted longitudinal waves. *Ultrasonics* 2015; 56: 417-426.
26. Matlack KH, Kim J-Y, Jacobs LJ, et al. Review of Second Harmonic Generation Measurement Techniques for Material State Determination in Metals. *J Nondestruct Eval* 2015; 34: 273.
27. Torello D, Thiele S, Matlack KH, et al. Diffraction, attenuation, and source corrections for nonlinear Rayleigh wave ultrasonic measurements. *Ultrasonics* 2015; 56:417-426
28. Walker SV, Kim J-Y, Qu J, et al. Fatigue damage evaluation in A36 steel using nonlinear Rayleigh surface waves. *NDT&E Int* 2012; 48: 10-15.

29. Jhang K-Y. Nonlinear Ultrasonic Techniques for Non-destructive Assessment of Micro Damage in Material: A Review. *Int J Prec Eng Manuf* 2009; 10: 123-135.
30. Cantrell JH. Quantitative assessment of fatigue damage accumulation in wavy slip materials from acoustic harmonic generation. *Phil Mag* 2006; 86:1539-1554.
31. Yan DW, Neild SA and Drinkwater BW. Modelling and measurement of the nonlinear behavious of kissing bonds in adhesive joints. *NDT&E Int* 2012; 47: 18-25.
32. Li W, Cho Y and Achenbach JD. Detection of thermal fatigue in composites by second harmonic Lamb waves. *Smart Mater Struct* 2012; 21: 1-8.
33. Shah AA and Ribakov Y. Nonlinear ultrasonic evaluation of damaged concrete based on higher order harmonic generation. *Mater & Des* 2009; 30: 4095-4102.
34. Matlack KH, Wall JJ, Kim J-Y, et al. Evaluation of radiation damage using nonlinear ultrasound. *J App Phys* 2012; 111: 1-3.
35. Liu M, Kim J-Y, Jacobs L, et al. Experimental study of nonlinear Rayleigh wave propagation in shot-peened aluminum plates – Feasibility of measuring residual stress. *NDT&E Int* 2011; 44: 67-74.
36. Müller MF, Kim J-Y, Qu J, et al. Characteristics of second harmonic generation of Lamb waves in nonlinear elastic plates. *J Acoust Soc Am* 2010; 127: 2141-2152.
37. Bermes C, Kim J-Y, Qu J, et al. Nonlinear Lamb waves for the detection of material nonlinearity. *Mech Syst Sig Process* 2008; 127: 638-646.
38. Mohseni H and Ng CT. Rayleigh wave propagation and scattering characteristics at debondings in fibre-reinforced polymer-retrofitted concrete structures. *Struct Health Monitor* 2018 https://doi.org/10.1177/1475921718754371.
39. Rose JL. *Ultrasonic Waves in Solid Media*. New York: Cambridge University Press,2004, pp.305-306.
40. Muir DD. One-Sided Ultrasonic Determination of Third Order Elastic Constants using Angle-Beam Acoustoelasticity Measurements. PhD Thesis, Georgia Institute of Technology, USA, 2009.
41. Jhang K-Y. Nonlinear Ultrasonic Techniques for Non-destructive Assessment of Micro Damage in Material: A Review. *Int J Prec Eng Manuf* 2009; 10: 123-135.
42. Thiele S, Kim J-Y, Qu J, et al. Air-coupled detection of nonlinear Rayleigh surface waves to assess material nonlinearity. *Ultrasonics* 2014; 54: 1470-1475.

43. Hermann J, Kim J-Y, Jacobs LJ, et al. Assessment of material damage in a nickel-base superalloy using nonlinear Rayleigh surface waves. *J App Phys* 2006; 99:1-7.
44. Viktorov IA. *Rayleigh and Lamb Waves: Physical Theory and Applications*. New York: Plenum Press, 1967, pp.8-9.
45. Hermann J. Generation and Detection of Higher Harmonics in Rayleigh Waves Using Laser Ultrasound. Master's Thesis, Georgia Institute of Technology, USA, 2005.
46. Hughes JM, Howie J, Vidler J, et al. Non-contact measurement of nonlinear Rayleigh waves using the scanning laser vibrometer. In: *9th Australasian Congress on Applied Mechanics*, Sydney, Australia, 27th-29th November 2017, pp.358-363.
47. Allen RL and Mills D. Time-Domain Signal Analysis. In: *Signal Analysis: Time, Frequency, Scale, and Structure*. 1st ed. New York: John Wiley & Sons, 2004, pp.338-341.
48. Bompan KF and Haach VG. Ultrasonic tests in the evaluation of the stress level in concrete prisms based on the acoustoelasticity. *J Construc Build Mater* 2018; 162:740-750.
49. Bra, DE and Tang W. Subsurface stress evaluation in steel plates and bars using the Lcr ultrasonic wave. *Nuc Eng Des* 2001; 207:231-240.
50. Li Z, He J, Teng J, et al. Internal Stress Monitoring of In-Service Structural Steel Members with Ultrasonic Method. *Struct Health Monitor* 2016; 9(4):223.
51. Li Z, He J, Teng J, et al. Absolute stress measurement of structural steel members with ultrasonic shear-wave spectral analysis method. *Struct Health Monitor* 2017 https://doi.org/10.1177/1475921717746952